TECHNICAL SUMMARY REPORT

STUDY OF PROPERTIES OF HIGH-FIELD SUPERCONDUCTORS AT ELEVATED TEMPERATURES

26 July 1965

Contract NAS 8-11272

Prepared by

APPLIED RESEARCH
DEFENSE ELECTRONIC PRODUCTS
RADIO CORPORATION OF AMERICA
CAMDEN, NEW JERSEY 08102

For

GEORGE C. MARSHALL SPACE FLIGHT CENTER
NATIONAL AERONAUTICS AND SPACE ADMINISTRATION
HUNTSVILLE, ALABAMA 35812

TECHNICAL SUMMARY REPORT

STUDY OF PROPERTIES OF HIGH-FIELD SUPERCONDUCTORS AT ELEVATED TEMPERATURES

26 July 1965

Contract NAS 8-11272

Prepared by

APPLIED RESEARCH
DEFENSE ELECTRONIC PRODUCTS
RADIO CORPORATION OF AMERICA
CAMDEN, NEW JERSEY 08102

For

GEORGE C. MARSHALL SPACE FLIGHT CENTER
NATIONAL AERONAUTICS AND SPACE ADMINISTRATION
HUNTSVILLE, ALABAMA 35812

FOREWORD

This report was prepared by the Radio Corporation of America as an annual report on the National Aeronautics and Space Administration contract NAS-8-11272, "Properties of High Field Superconductors at Elevated Temperatures." Work was administered under the direction of the George C. Marshall Space Flight Center, National Aeronautics and Space Administration. Mr. E. W. Urban was project engineer for NASA.

The Applied Research department of RCA in Camden, New Jersey, in collaboration with the David Sarnoff Research Center in Princeton, N. J., performed the work covered by this report during the period from June 21, 1964 through June 21, 1965.

This report was prepared by R. Hecht and C. M. Harper, who were the principal investigators.

ABSTRACT

An experimental program to study the current-carrying capacity of high-field superconductors at elevated temperatures is described. Currents are induced in the windings of shorted NbZr and Nb_3Sn coils, or in the walls of NbZr, Nb_3Sn and NbTi tubes, by applying a magnetic field parallel to the sample axis. The critical current density, J_c, is then found to depend on temperature, applied field (applied field sweep rate) and on the defect structure of the superconductor. It is found that various mechanisms will trigger the sudden revision of a sample to the normal state, (flux jump), but that a particular mechanism will dominate in a given sample under given experimental conditions.

Author

TABLE OF CONTENTS

SECTION I

INTRODUCTION

The purpose of studying the properties of high-field superconductors at elevated temperatures is to determine the conditions under which magnets and superconducting shields can operate stably and reproducibly. Indeed, no loss in high-field J_c may be entailed in such operation; it is in principle possible to program an increasing current and decreasing temperature so as to avoid the low-field, low-temperature region of instability. Furthermore, high-temperature operation might be necessary under conditions where the weight and power requirements of a helium liquifier, or the absence of a gravitational field, would be important considerations.

The method employed in these studies is to induce current in the walls of superconducting tubes, or in the windings of shorted superconducting coils, by applying a magnetic field parallel to the sample axis. In this way, intense current densities ($\sim 10^6$ A/cm^2) can be induced without introducing external leads. These currents can be inferred by measuring the field within the sample bore. Measurements have also been made on J_c in externally fed coils, but this method involves severe technical difficulties. In particular, the joint between the superconductor and the normal lead is exposed to the full heat flow down the lead.

A. CRITICAL CURRENTS

High-field superconductors, such as the niobium-based alloys commonly employed in commercial superconducting solenoids, have properties differing markedly from those of soft superconductors such as lead or tin. In particular, applied magnetic fields will penetrate a high-field superconductor without destroying its

ability to support supercurrents. For Nb_3Sn this penetration occurs at an applied field strength perhaps one hundredth of that required for the complete destruction of superconductivity. In this so-called "mixed state", bulk transport currents can be maintained within the superconductor.

The critical current density, J_c, that the high-field superconductor can carry without reverting to the normal state is known to depend both on temperature and on local magnetic field intensity. To a considerable extent, J_c will also depend on (1) the defect structure of the superconductor, (2) the relative magnitudes of the thermal and electrical diffusivities (this bears on the stability of the material against the formation of hot spots), (3) the rate at which changes in field or temperature are effected and (4) the treatment of the sample surface.

It is also commonly observed that the critical current which can be carried by an isolated length of wire is, at low applied fields, substantially higher that that for the same wire when wound into a solenoid which generates an equal field. This last phenomenon is of considerable practical importance, and is still imperfectly understood. The general belief is that erratic field changes in a given section of wire will influence the state of neighboring sections, leading to a cooperative breakdown of superconductivity.

It has been found that such measures as coating the wires with good normal conductors or interleaving sheets of good normal conductors between solenoid layers tend to damp this regenerative process. Also, this low-field region of instability may be avoided in a compound solenoid by applying sufficient field to the inner sections before energizing them with current.

B. TUBE MAGNETIZATION

Considerable insight into the behavior of superconducting solenoids, as well as information about J_c for a given material, can be obtained from a study of the magnetization of superconducting tubes. It is commonly found for those high-field

superconductors which are rich in defects that the magnetization is strongly hysteretic and size-dependent. For such cases, Bean[1] suggests a model in which bulk screening currents extend from the surface inwards, maintaining a constant critical density J_c, to whatever depth is necessary to shield the interior from an increasing applied field. On reducing the field, a second current sheath of opposite sign extends from the surface inwards, not merely erasing but reversing the earlier current distribution throughout the depth to which the second sheath penetrates. Hysteresis is thus seen to be an immediate consequence of this model. It also follows that a rod of such material will have a saturation magnetization, M, proportional to its radius, R ($M = RJ_c/3c$ expressed in esu). A more refined model, in which J_c depends on the local magnetic field intensity, is used by Kim, Hempstead and Strnad[2] to analyze their extensive observations of the magnetization of NbZr and Nb_3Sn tubes.

C. KIM-ANDERSON THEORY

Kim and Anderson[3] have shown that the probable source of these bulk screening currents is the presence of gradients in the density of Abrikosov vortices. These vortices are narrow (~ 1000Å) tubes composed of azimuthal currents generating a quantum $\varphi_o \approx 2 \times 10^{-7}$ gauss-cm^2 of flux, and they propagate inwards from the surface when the superconductor enters the mixed state. A gradient in the vortex density supplies the magnetic pressure differential necessary to move the vortices past pinning sites at an observable rate. Conversely, it is the pile-up of vortices at pinning sites which establishes the gradient. Accordingly, wherever flux has moved a critical gradient remains whose value depends on temperature, vortex density and vortex interaction strength, and on the defect structure of the superconductor. Critical current J_c is then seen to be roughly the product of the vortex density gradient and the quantity $c\varphi_o/4\pi$, a more exact expression requiring a lengthly thermodynamic treatment.[4]

D. FLUX JUMPING

A phenomenon which is readily interpretable in terms of the Kim-Anderson theory is the "flux jump". This is a catastrophic reversion of a magnetized superconducting sample, say a tube, to the normal state. The sample then rapidly returns to the superconducting state, but the wall current and accompanying magnetization have vanished.* Flux jumping is quite similar to the phenomenon of "quenching" in high-field solenoids, and is observed to occur only at modest fields and low temperatures, and to depend on material, sample dimensions and surface treatment. The Kim-Anderson theory accounts for a flux jump as an avalanche in which heat which is generated by the motion of vortices supplies the activation energy which liberates other vortices from their pinning sites.

Flux jumping ceases at sufficiently high fields due to the reduction in the vortex density gradient; it ceases at sufficiently high temperature due to the increase in thermal conductivity and to the reduction of the low field vortex density gradient. One purpose of the present studies is to map out the boundaries, in the field vs. temperature domain, within which flux jumping behavior is confined. It should be noted that flux jumping can be induced outside these boundaries by too rapid a variation of applied field or of temperature, but even with quasi-static variation it persists within them, and may be considered a fundamental property of the sample.

---

*It is conventional to define tube magnetization M in terms of the difference between the applied field H and the bore field H'. Thus, $4\pi M = H' - H$. The wall itself is in general magnetized, in that the induction B in the wall differs from H.

SECTION II

APPARATUS AND TEST PROCEDURE

The equipment used to test high-field superconductors at elevated temperatures consists of a cryostat, a field source (superconducting solenoid), a heater cavity and field and temperature sensors. Figure 1 shows the test setup during a typical experiment. The cryostat is in the foreground. The rack of test equipment on the left contains (1) an x-y recorder on which magnetization is plotted against field, (2) a current supply for the superconducting solenoid, (3) a digital voltmeter and (4) a millimicrovoltmeter. The tray of test equipment in the background holds the battery power supplies, ammeters, and level controls for a Hall probe, for germanium resistance thermometers, and for the heater which surrounds the sample. The valves on the right control a vacuum pump.

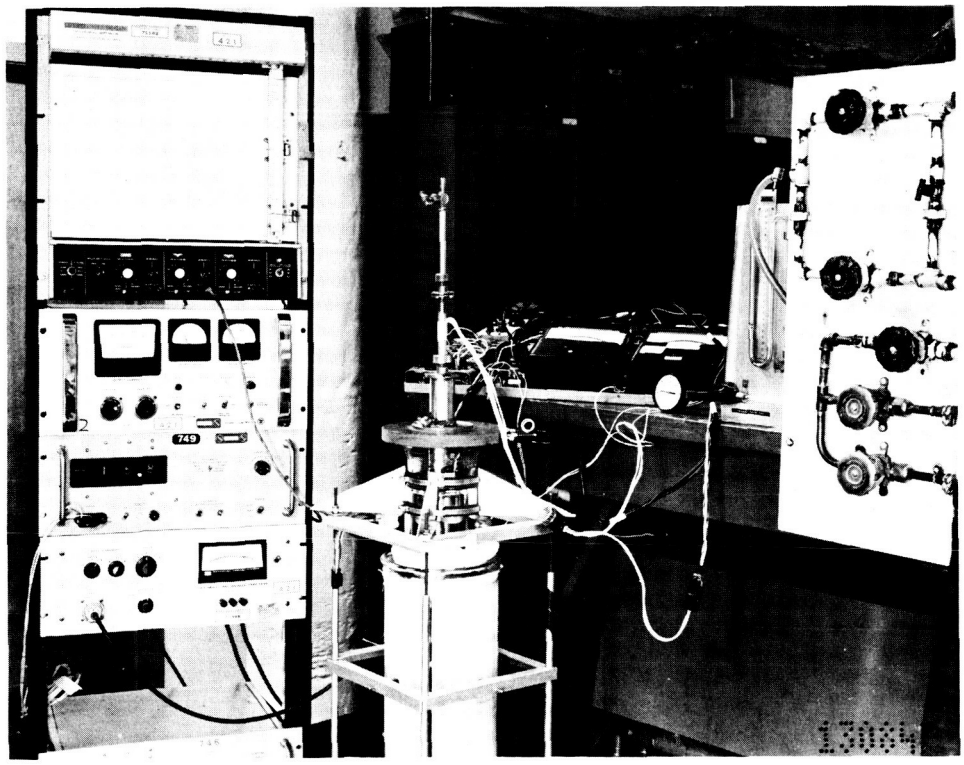

Figure 1. Apparatus for testing high-field superconductors at elevated temperatures.

The components contained in the cryostat are shown in Figure 2. The superconducting solenoid at the top generates a field of 27,000 gauss in a 1.5-inch bore. The solenoid has 13,400 turns of 0.010-inch NbZr wire clad with 0.001-inch of copper and insulated with formvar. Below the solenoid is the heater cavity with a sample holder inserted. The heater cavity is a 7-inch length of 0.875-inch stainless steel tubing mounted at the end of a 45-inch support of 0.5-inch stainless steel tubing. The cavity is insulated from the surrounding liquid helium bath by a 0.125-inch-thick jacket of nylon, with additional insulation provided by layers of teflon tape which extend for about one foot up the support tube. Leads are introduced to the heater cavity through a multi-pin glass seal which closes its lower end.

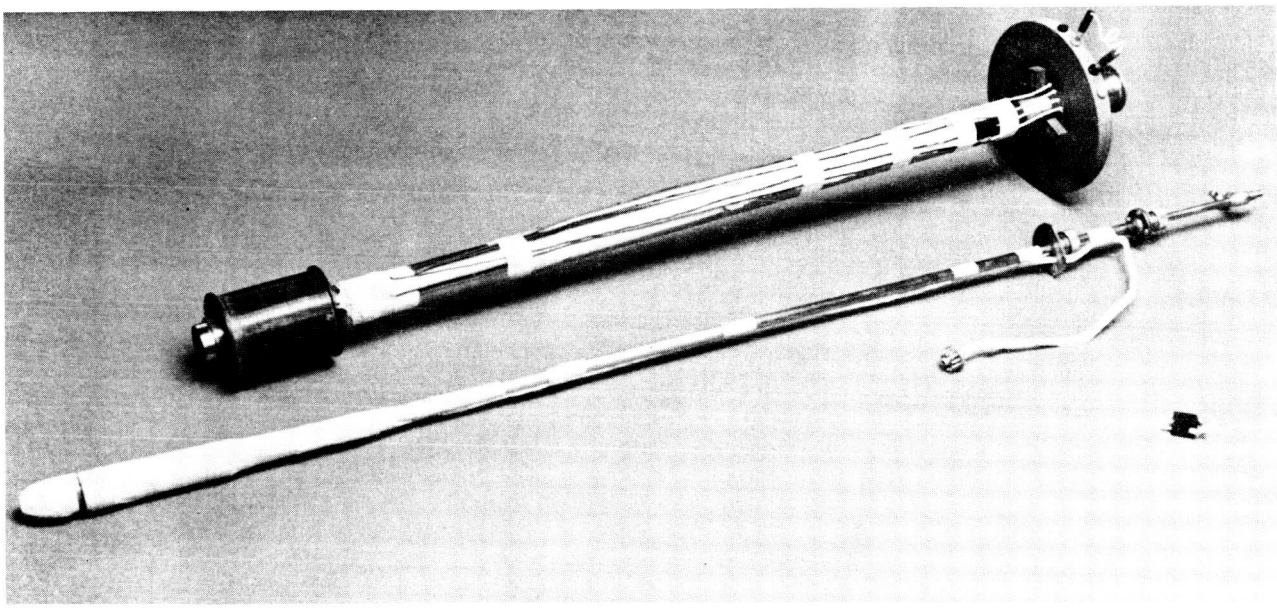

Figure 2. 30-kG solenoid and heater cavity.

Figure 3 is a cut away view showing the inside of the heater cavity as it would look with a sample partially inserted. Samples are supported in a perforated bakelite holder at the end of a stainless steel tube. As a sample is lowered into the cavity, it comes to rest with the Hall probe centered inside the sample and with

the vacuum flange of the sample holder tube mating with the vacuum flange of the heater cavity support tube. With the sample in place, the heater cavity assembly is then flushed with helium gas, evacuated to about one torr through the valve at the top of the sample holder, and pre-cooled in liquid nitrogen. The solenoid is separately pre-cooled and placed in the cryostat, liquid helium is transferred, and the heater cavity is then lowered into the center of the solenoid. To change samples during a run, the heater cavity must be removed from the cryostat to avoid condensation.

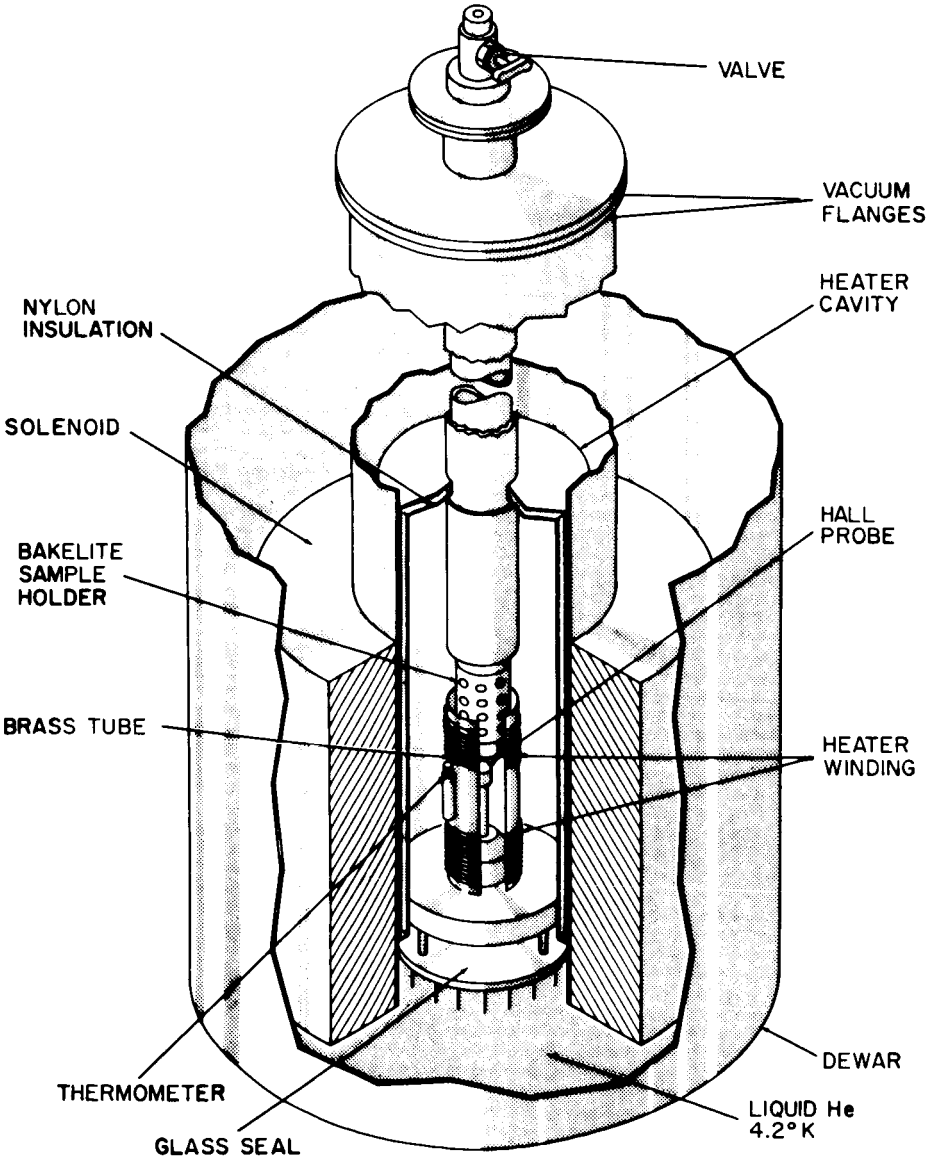

Figure 3. Cross-sectional view of apparatus.

The heater is a bifilar winding of manganin wire on a brass sleeve which surrounds the perforated bakelite sample holder. A calibrated germanium thermometer is mounted midway along the brass sleeve. Using a thermometer current of 10 μ A, the voltage developed across the thermometer is amplified by the millimicrovoltmeter and displayed on the digital voltmeter. The relation of sleeve thermometer voltage to sample temperature has been established by tests made with a second thermometer inserted into the sample space. There was some difficulty first in obtaining a reproducible determination of sample temperature from sleeve temperature. One reason for this appeared to be convection of heat in the tubes supporting the sample holder and heater cavity. The practice of evacuating the heater cavity has largely eliminated this problem, and the temperatures of sample and sleeve now track consistently to within an uncertainty of about 0.1°K.

The same millimicrovoltmeter which amplifies the sleeve thermometer output is also needed to amplify the output of the Hall probe which senses the field inside the sample. Therefore temperature cannot normally be monitored continuously. However, having fixed the heater power, a steady temperature is shortly reached which remains stable to within 0.1°K for several minutes. Since this temperature drift is at most of the order of the tracking error between sleeve and sample temperatures, it has not seemed necessary to monitor temperature more frequently or to take steps to introduce automatic regulation.

The Hall voltage amplified by the millimicorvoltmeter then drives the y-axis of the x-y recorder. The current to the superconducting solenoid passes through a series meter shunt which drives the x-axis of the x-y recorder. In this way, plots are obtained of the field inside the sample, H', against the applied field, H.

SECTION III

EXPERIMENTAL INVESTIGATION

A. TUBE MAGNETIZATION

1. General

As outlined in the introduction, the magnetization of superconducting tubes can be described in terms of the Bean[1] model (J_c constant), or still better, in terms of the model employed by Kim, Hempstead and Strnad[2] (J_c field dependent). When a field H is first applied to a superconducting tube, the field H' within the tube bore is maintained at H' = 0 by the flow of currents in the tube wall. Thickness, x, of the current layer is determined by the equation

$$H = 0.4\,\pi\,J_c x$$

or by an equivalent integral equation if J_c is taken to vary with field within the wall. Here H is in gauss, J_c is in amperes per square centimeter, and x is in centimeters. As H increases so will x, until (assuming that flux jumping does not intervene) the entire wall is carrying its critical current, J_c. The magnetization $M = (H' - H)/4\,\pi$ is then saturated, and on further increasing the field, H' will increase with H. The sample is then said to be in the "critical" state.

If, as is ordinarily the case, J_c decreases with increasing field, H' will increase faster than H, and the magnetization will approach zero. Kim, et al[2], have proposed a semi-empirical relation

$$J_c = \frac{\alpha_c}{H^* + B_o} \qquad (1)$$

to describe the variation of current with field in the critical state. Here H* is the mean field in the tube wall and α_c and B_o are adjustable parameters. It can be

seen that α_c has the dimension of a force; it may be interpreted to be the critical Lorentz force needed to overcome pinning forces and to allow flux to move across the tube wall. Given a wall thickness, w, it follows providing Equation 1 holds that

$$H - H' = \frac{0.4\pi\omega\alpha_c}{B_o + H^*} \tag{2}$$

It is then convenient to plot values of $(H - H')^{-1}$, obtained from a critical state magnetization curve, against $H^* = \frac{1}{2}(H + H')$. The value of α_c can then be obtained from the slope of the plot, and the value of B_o from the intercept at $H^* = 0$ That is,

$$(0.4\pi\omega\alpha_c)^{-1} = \frac{d}{dH^*}\left[(H - H')^{-1}\right] \tag{3a}$$

and

$$B_o = \lim_{H^* \to 0} \frac{0.4\pi\omega\alpha_c}{H - H'} \tag{3b}$$

To the extent that such a plot is linear, Equation 1 may be said to describe the field dependence of J_c. We confirmed this form of field dependence at low temperatures for all our samples, but at higher temperatures it will be seen that J_c decreases with field substantially faster than H^{-1}.

If a tube has been magnetized to the critical state by increasing the field, and the field is then reduced, H' will be held constant by a second current layer of opposite sign to the original current distribution. This second layer extends inward from the surface, exactly as did the first, to a depth x such that $\Delta H = 0.4\pi J_c x$, where ΔH is the amount by which the original field has been reduced. When the second current layer completely fills the tube wall, the sample is again in the critical state with respect to the decreasing field. As the field decreases further, J_c grows, and at H = 0 a remanent magnetization (trapped field) exists.

Figure 4 illustrates the nature of critical state behavior, and also of flux jumping. The data were obtained with a NbZr tube 1.25 inches long, 0.25 inch in

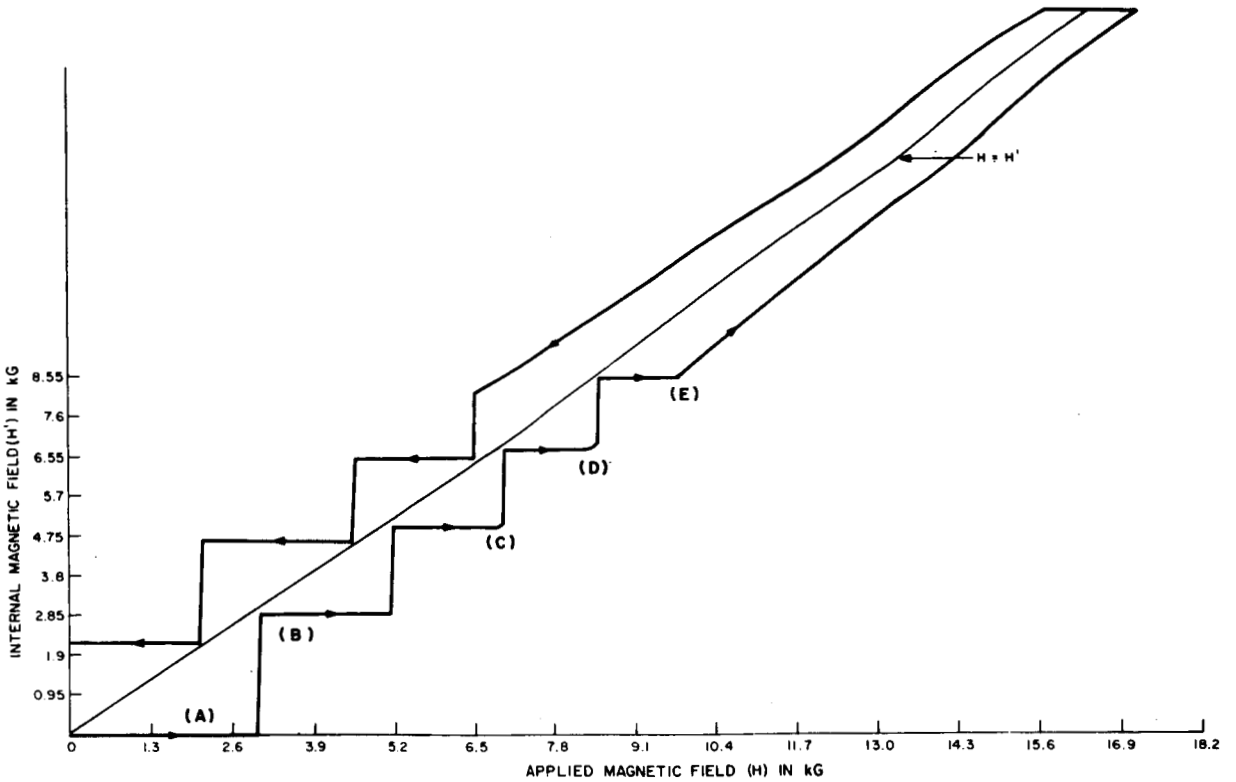

Figure 4. Magnetization of NbZr tube at 6.2°K.

diameter, and 0.050 inch in wall thickness. H' was monitored with a Hall probe. Referring to Figure 4, note that as H is increased from H = 0 (along line A) no change in H' occurs until a flux jump drives the sample normal (point B). The sample then rapidly* cools to the superconducting state, maintaining constant the field H' which entered at the flux jump. Flux jumps continue, sometimes following intervals in the critical state (points C and D). At still higher fields (following point E) the critical state appears stable against further flux jumping. When the field is reduced, H' remains constant until J_c has been completely reversed, then decreases with field, and finally enters the low-field flux jumping region.

*The time constant L/R for the tube in the normal state is estimated to be about 100 μ s. For the field sweep rate $dH/dt \approx 200$ G/s ordinarily used, the shielding $(L/R)(dH/dt)$ would be negligible in the normal state, and the magnetization would follow the H' = H curve during any normal interval. Since no such interval is observed, we estimate the normal to superconducting return time to be less than the time resolution of our recorder, which is perhaps 0.1 s.

2. Flux Jumping in Nb_3Sn and NbZr Tubes

In most of the Nb_3Sn samples studied, the critical state was never established (even briefly) at temperatures near 4.2°K, within the 30 kG field available. This must be contrasted with the observations of Kim, Hempstead and Strnad[2] and of McEvoy[5], who were generally able to establish the critical state without difficulty at 4.2°K and at fields of a few kG. We attribute this to the fact that our samples were not immersed in a liquid helium bath. In discussing the magnetization of such samples, we will refer to the "practical" magnetization and "practical" current density which exist immediately prior to a flux jump. The "practical" current density is defined as the current per unit length, divided by wall thickness w, and is less than or equal to the true current density (which may actually flow in a layer thinner than w.)

Figure 5 shows the "practical" magnetization for an Nb_3Sn tube (sample PM 24#4). This tube is about 1.25 inches long, 0.25 inch in diameter, and has an 84-micron wall deposited on a ceramic substrate. Up to temperatures of about 7.5°K, the sample did not exhibit critical state behavior (smoothly decreasing magnetization with increasing field) but rather showed flux jumps whose size decreased with increasing field or with decreasing temperature. No significant change in flux jumping pattern was noted on decreasing the field sweep rate from 200 G/s to 75 G/s. At about 7.5°K, brief intervals of critical state behavior were observed prior to flux jumping. Above about 10°K, almost pure critical state behavior occurred, sometimes with one or two flux jumps at low fields.

The solid curves in Figure 5 were drawn through those points at which flux jumping occurred at temperatures above 7.5°K. In addition, the initial flux jumps occurring at temperatures below 6.9°K are plotted as single points. The full curves for these lower temperatures are not shown since they are less regular and reproducible than the solid curves shown for higher temperatures. We suspect that at these higher temperatures (above 7.5°K in Figure) flux jumping occurs close to the onset of the critical state, i.e., at the point where the entire wall is carrying critical current.

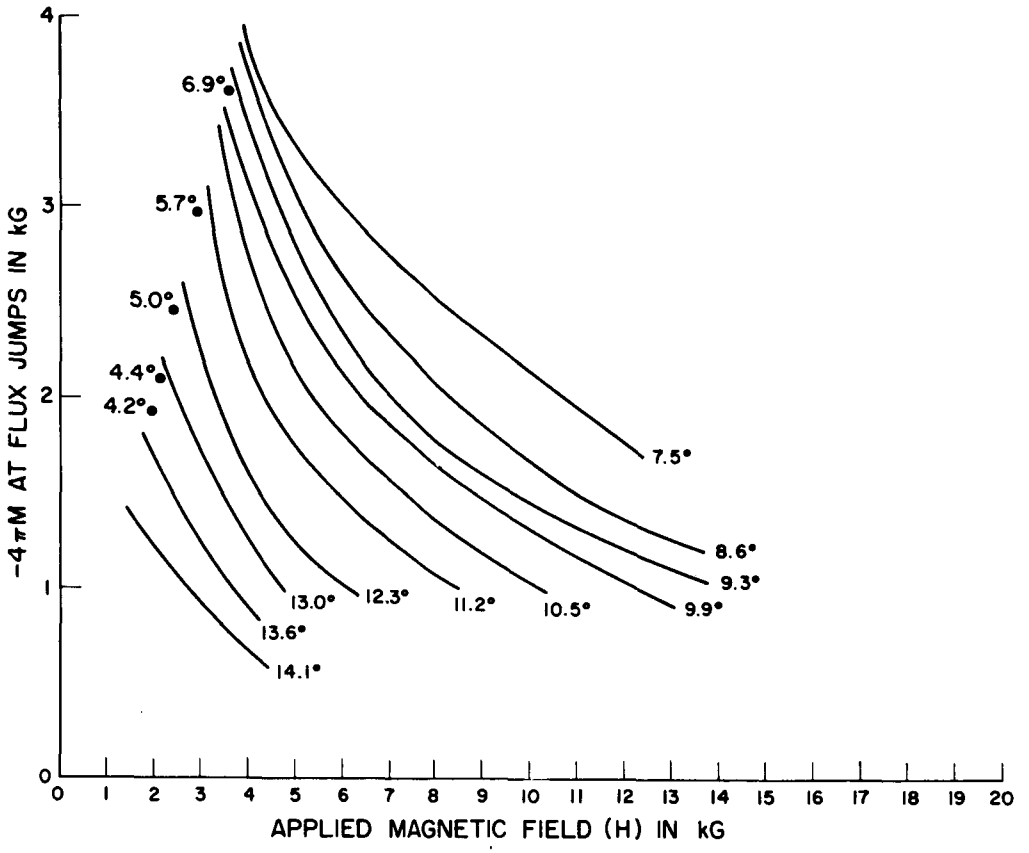

Figure 5. "Practical" magnetization of Nb_3Sn tube.

In the critical state, vortices are created in increasing fields at the tube outer surface, move across the tube wall, and are destroyed at the inner surface. It may be that the heat given up by the destruction of a vortex at the inner surface triggers the flux jump, provided that the gradient in vortex density is sufficiently steep. At lower temperatures (below 6.9°K in Figure 5)., it seems clear that the wall is not fully penetrated by current at the point where a flux jump occurs.

If the values of "practical" magnetization shown in Figure 5 are converted to "practical" current densities, and are replotted against temperature at fixed field, curves like those shown in Figure 6 are obtained. The region below 7°K in Figure 6 is not shown in Figure 5; it is an estimate made by smoothing out the erratic "practical" magnetization observed at these temperatures. It can be seen that the "practical" critical current density for this sample peaks at roughly 7.5°K

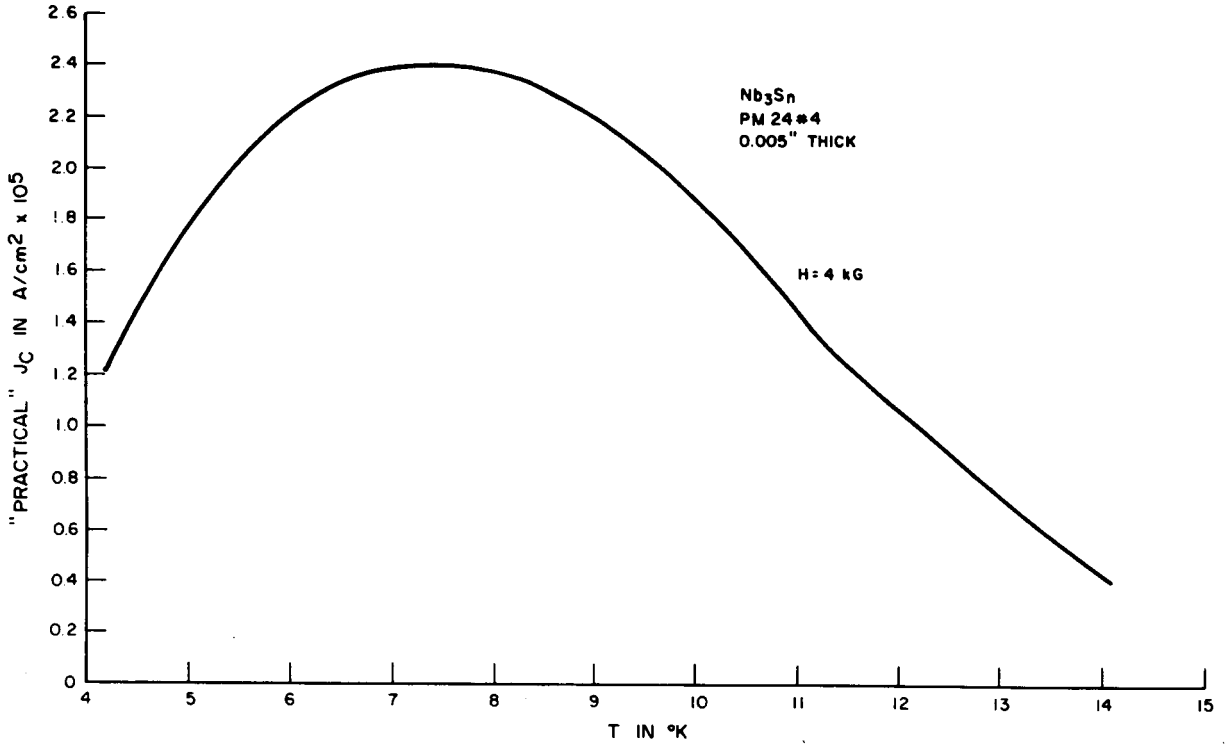

Figure 6. "Practical" J_c of Nb_3Sn tube.

at an applied field of 4 kG. This is not to say that the location of the peak is fundamental to this material; it seems likely that a thinner walled sample would peak at a lower temperature and a thicker walled sample at a higher temperature.

Figure 7 shows, for representative NbZr and Nb_3Sn tubes, those regions in field and temperature within which the critical state is unmarred by flux jumping. The left-hand boundary of each shaded region is obtained by plotting that field value at which the final flux jump occurred for a given temperature (for example, point D in Figure 4). The right-hand boundary of each shaded region is assumed to be the upper critical field for each material, whose slope we take to be roughly 10 kG/deg. The data suggest that the slope of the left-hand boundary is increasing indefinitely as the temperature decreases; this would indicate that for these samples, flux jumping will persist to the upper critical field, for all temperatures below the temperature at which the left-hand boundary is vertical.

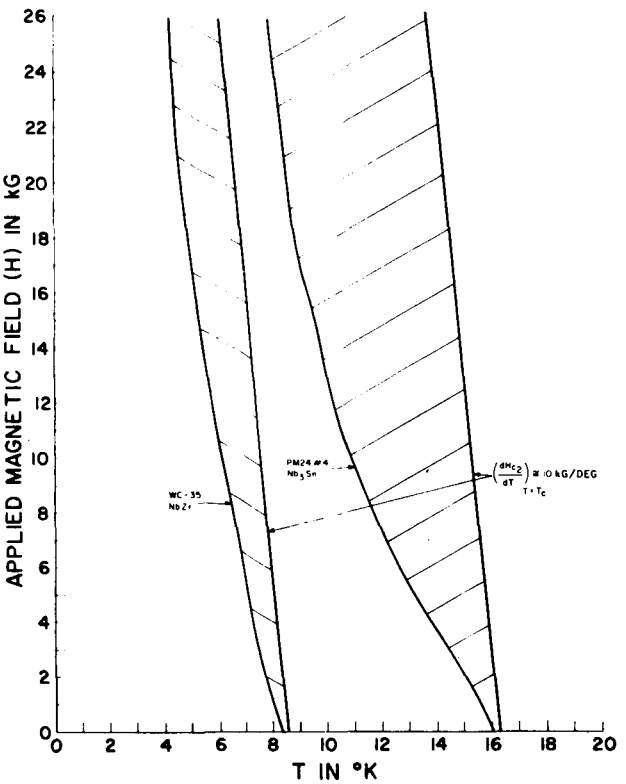

Figure 7. Regions of critical state for Nb_3Sn and NbZr tubes.

3. Magnetization of NbTi Tubes

Two samples of NbTi (alloy HI 120) were obtained from Westinghouse. As purchased, the samples were in the form of tubes, 1.25 inches long, 0.25 inch O.D., and 0.050 inch in wall thickness. The degree of cold-work was estimated by Westinghouse as about 75 percent. The samples, hereafter identified as HI-1 and HI-2, were from the same ingot.

J_c was measured for both samples, and agreed closely between them. A complete set of magnetization plots for different temperatures was obtained for HI-2, Figure 8 being a typical plot. The critical state is seen to lie along the dashed line, and solid line above point D, in Figure 8. It was observed that when the rate of change $\frac{dH}{dt}$ of applied field was reduced to about one G/s, all flux jumping could be avoided even at temperatures near 4.2°K (See the region in the vicinity

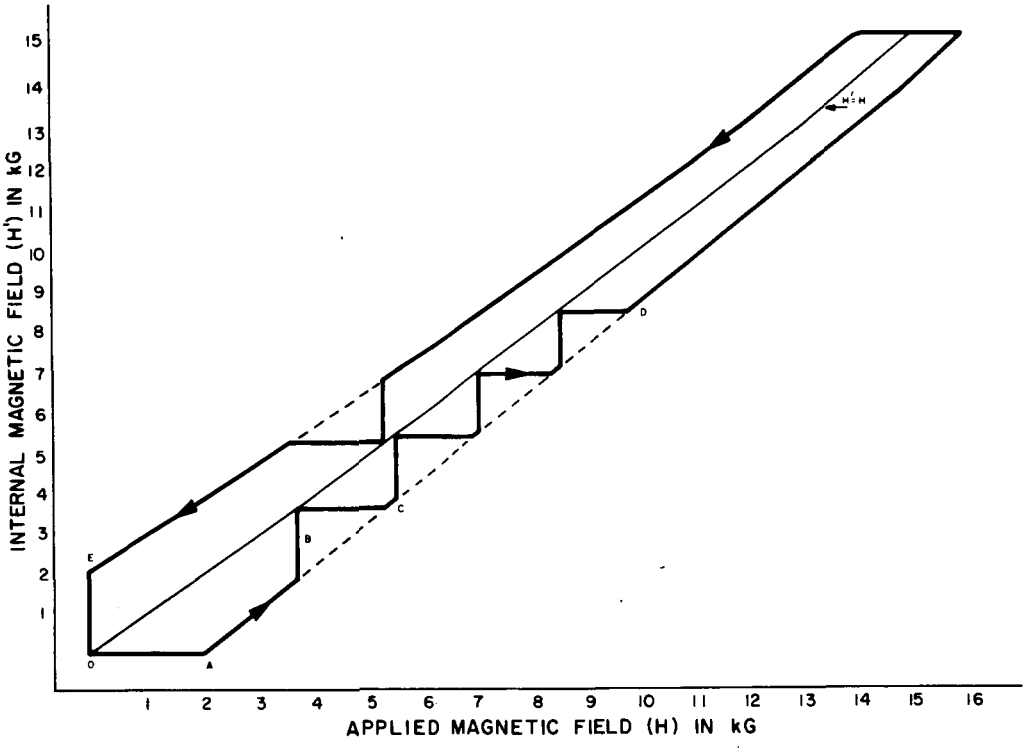

Figure 8. Magnetization of NbTi tube at 6.2°K.

of point A in Figure 8.) The flux jumps observed in Figure 8 occurred at a sweep rate $\frac{dH}{dt} = 200$ G/s. This behavior is quite different than that observed for Nb_3Sn, which exhibited flux jumping patterns independent of sweep rate below $\frac{dH}{dt} = 200$ G/s until the temperature was raised to about 8°K. Even at higher temperatures, flux jumping in Nb_3Sn depends less on $\frac{dH}{dt}$ than it does for these samples of NbTi. In explanation, it is generally understood that the defect structure of freshly cold-worked NbTi is homogeneous, and defect clusters large enough to effectively trap vortices are scarce. In this regard, it will be seen that these samples have relatively low values of J_c, and that mild heat-treatment, leading to an agglomeration of defects, raises J_c. Thus, in the untreated cold-worked material, conditions for flux jumping (viz, steep vortex density gradients) are not ordinarily present, provided that flux is not driven by too rapidly changing the applied field.

Plotting the critical state magnetization for these samples in the manner described in the text following Equation 2, one obtains the family of curves shown

in Figure 9. It can be seen that the curves are linear (i.e., they satisfy Equation 2) below about 7°K, and are increasingly nonlinear above 7°K. A similar deviation, but to a lesser degree, was noted for Nb_3Sn. Evidently, at higher temperatures J_c decreases (with increasing field) faster than the reciprocal of the applied field. This is in general agreement with the results of Cody and Cullen[6], who find for Nb_3Sn that $J_c \propto (H)^{-1.5}$ near T_c.

For comparison with the data obtained with untreated cold-worked NbTi, one of the samples HI-1 was partially annealed at 400°C for 2.5 hours in a vacuum of 3×10^{-6} torr. Following this treatment, J_c for this sample increased five-fold; furthermore, the sample showed a much increased tendency to flux jump over the entire temperature range from 4.2°K to T_c. Figure 10 shows the limiting low-field critical state values of J_c for this material obtained before annealing, and the "practical" low-field values of J_c obtained both after annealing and after temperature cycling the annealed sample from room temperature to 4.2°K. The degradation of the "practical" J_c after temperature cycling is undoubtedly the result of thermal stressing.

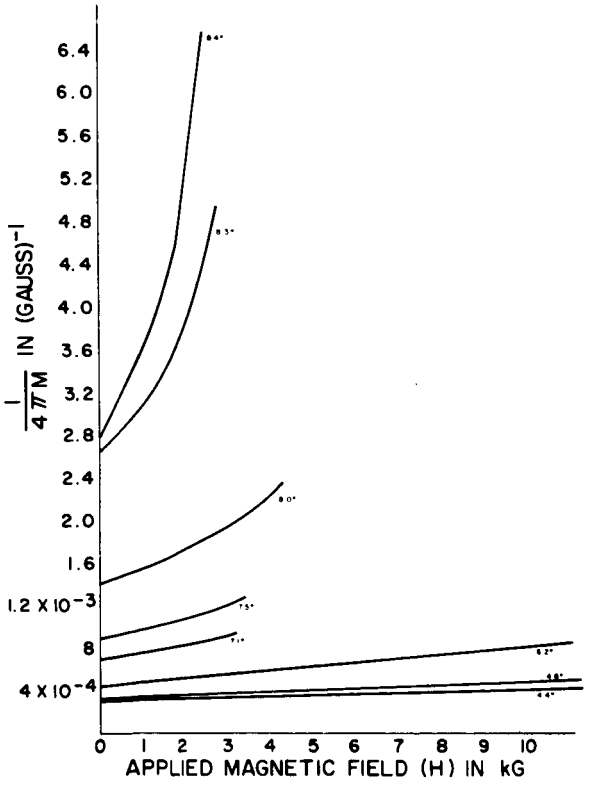

Figure 9. Reciprocal of tube magnetization for NbTi tube.

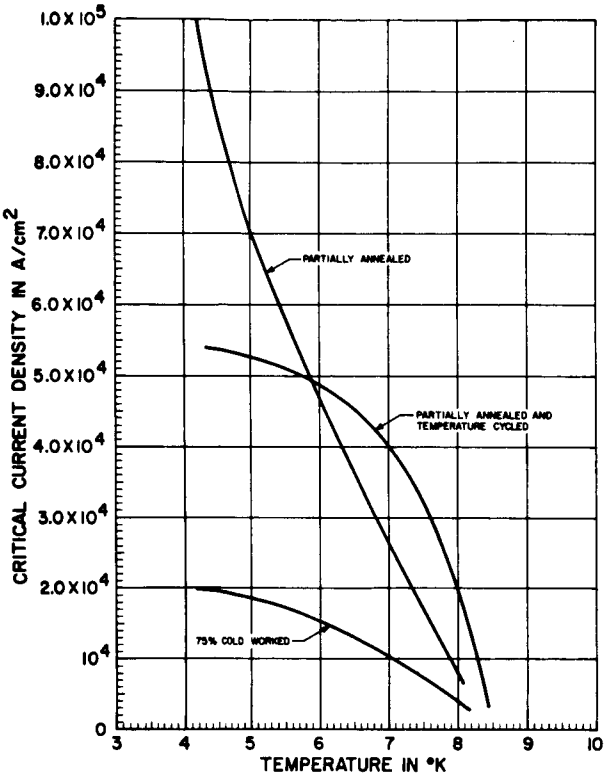

Figure 10. Critical current density of NbTi tube.

B. MAGNETIZATION OF COILS

1. Shorted Solenoids

Measurements were made of the fields H' within the bores of three shorted superconducting solenoids. Applied fields H ranged up to 30 kG, and sample temperatures ranged from 4.2°K up to T_c.

The first solenoid (NbZr #1) was 3 cm long, 0.55 cm in I.D., and 1.0 cm in O.D. The Westinghouse NbZr wire used had a 0.005-inch core, a 0.001-inch-thick copper cladding, and an outer 0.001-inch-thick fused nylon insulation. The solenoid had 9 layers and a total of 1080 turns. To short this solenoid, the leads were brought out for a length of 4 inches so that the joint would be in a weak field ($\sim 2\% H_{max}$). After cleaning down to bare NbZr, the wires were spot-welded to a sheet of NbZr. It will be shown that the joint is superconducting.

The second solenoid (Nb_3Sn #2) was 3 cm long, 0.8 cm in I.D., and 1.0 cm in O.D. The RCA tape used was 0.025 inch wide, 0.003 inch thick, with a 0.0005-inch-thick deposit of Nb_3Sn. The tape has an outer copper cladding 0.0005 inch thick. The solenoid has 3 layers and a total of 150 turns. To make the short, the leads were brought out as described above, but because Nb_3Sn is an intermetallic compound, an initial attempt at spot-welding was unsuccessful. To overcome this difficulty, the leads were soft-soldered together without removing the copper cladding. The resulting joint had a resistance which is estimated, from the results below, to be about 2×10^{-6} ohm. This may be compared with the resistance of the welded joint which was similarly estimated to be about 10^{-3} ohm.

The third solenoid (Nb_3Sn #3) had the same dimensions as solenoid Nb_3Sn #2, but had 112 turns. The RCA tape was 0.090 inch wide with a 0.0005-inch-thick deposition of Nb_3Sn, and it was clad with silver. The silvered surfaces of the ends of the tape were soldered with 60-40 lead-tin solder with a cool iron. The resistance of the shorted joint was estimated to be of the order of 2×10^{-8} ohm.

To analyze the performance of these solenoids, consider first the voltage V induced in a single turn of wire with radius r; it is

$$V = -10^{-8} \frac{d}{dt} \left\{ \pi r^2 H + \Phi_{ind} \right\} \tag{4}$$

where H is the applied magnetic field, and Φ_{ind} is the flux due to the induced current I. The constraint equation is then

$$\sum_{\text{all turns}} V = IR \tag{5}$$

where R is the total series resistance (resistance of short). Evaluating Φ_{ind} for all turns and performing the summation (Eq. 5) is a tedious process for solenoids of finite length; fortunately, the necessary results have been published recently.[7]

Noting that for R = 0, Eq. (5) yields

$$\sum_{\text{all turns}} \left\{ \pi r^2 H + \Phi_{\text{ind}} \right\} = \sum_{\text{all turns}} \pi r^2 H_o, \qquad (6)$$

we obtain from Reference 7 (using the dimensions of solenoid NbZr #1) the value of $H' = H_o - 0.36H$. Here H_o is the field present when the solenoid goes superconducting (say after a flux jump), and it is initially zero. To understand the fact H' decreases with increasing H, note that the total flux linked by the solenoid is conserved. Further, since the field in the outside windings increases with H (see inset in Figure 11), the field in the inner windings and bore must decrease with H. Figure 11 is a plot of H' versus H, which is typical of the results obtained below about 7°K. The predicted inductive behavior is confirmed quite closely, except where interrupted by flux jumping.

Above 7°K, critical state behavior is observed. The current limits itself to a value I_c (after several initial flux jumps) so that the H'-vs-H plot is quite similar in appearance to the observed critical state plots for tubes. An interesting effect occurs in solenoids, however. Whereas critical state behavior in tubes is interrupted by occasional flux jumps, critical state behavior in this shorted solenoid (NbZr #1) is interrupted by brief intervals of inductive behavior during which the current increases (see Figure 12). We interpret this behavior by noting that Type-II superconductors carrying current in large fields develop voltages along the current flow direction.[2] This voltage results from the motion of vortices; hence; there is an equivalent series "resistance". (An analysis of the performance of a superconducting solenoid with a finite resistance short (NbSn #2) is given below). Should vortex motion be temporarily impeded, the "resistance" disappears and the solenoid reverts to inductive behavior.

Attention should be drawn to the nature of the flux jumps which occur in the shorted NbZr solenoid (NbZr #1). At low temperatures (see Figure 11) the jumps occur regularly at a spacing which decreases as the field increases, the current

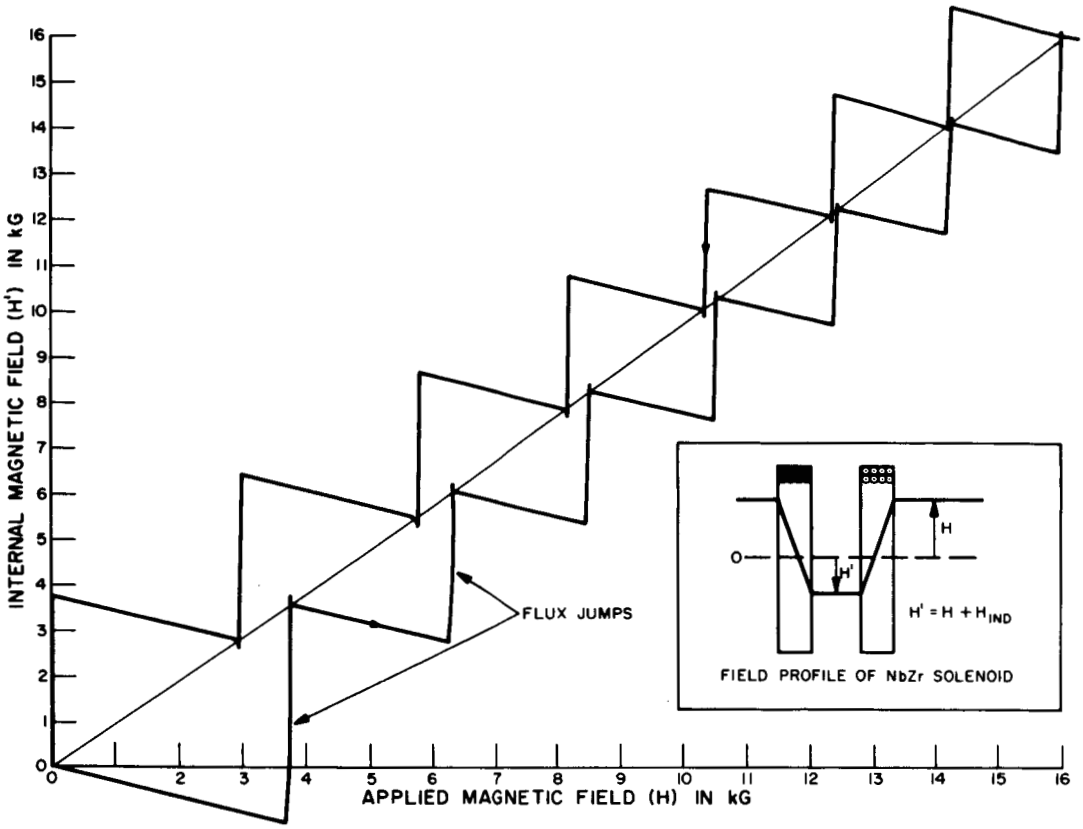

Figure 11. Magnetization of NbZr solenoid at 5.4°K.

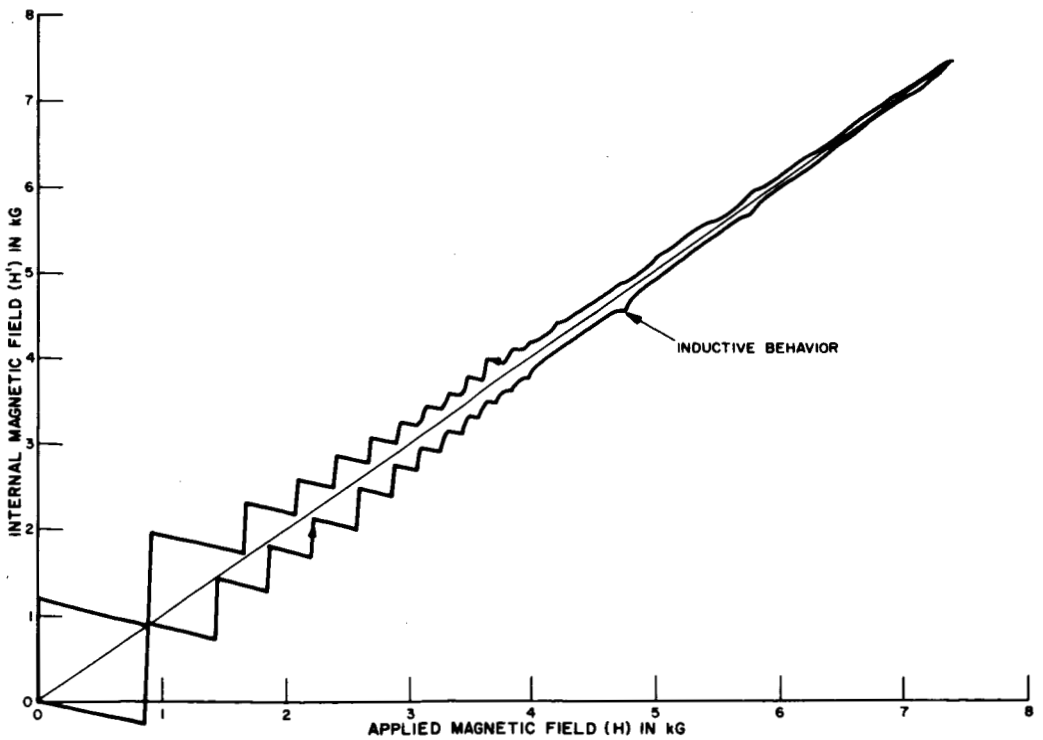

Figure 12. Magnetization of NbZr solenoid at 7.6°K.

is completely destroyed by the jump, and there is no trace of critical state behavior, i.e., no trace of current saturation. At higher temperatures (see Figure 12), the jumps at first occur regularly but with a smaller spacing than at low temperatures, the current is not completely destroyed for jumps at fields above 2 kG, and the jumps finally are reduced to small field excursions about what is essentially critical state magnetization. Also, the jumps at high as well as low temperatures always follow an interval of inductive behavior, as evidenced by the negative slope of the magnetization preceding the jump. It seems clear that for this sample a jump occurs only when flux is not flowing; in the critical state region flux must stop flowing before a jump occurs. We will wish to compare this behavior with that of the Nb_3Sn solenoids described below.

Figure 13 shows the critical current and critical current density for solenoid NbZr #1 at the initial flux jump as a function of temperature. It should be noted that the critical current decreases almost linearly with temperature, whereas in thick-walled NbZr tubes, the critical current at the first flux jump has a maximum at some intermediate temperature. The difference can be understood by noting that in tubes, the thickness of the current layer at the first flux jump can be much less than the wall thickness, and it increases progressively with temperature. In solenoids, the current density is uniform throughout the windings.

We now consider the two Nb_3Sn solenoids which had finite resistance shorts. For a long, thin-walled solenoid of inductance L and finite resistance R, the solution to Equations 11 and 12 is found to be

$$H' = H - \frac{L}{R}\frac{dH}{dt}\left[1 - \exp\left(-Rt/L\right)\right] \qquad (7)$$

where the field sweep rate, dH/dt, is taken to be constant. Figures 14 and 15 are plots of H' versus H for solenoid NbSn #2. These plots have several distinctive features. The initial dependence of H' on H follows Equation 7, provided $R \approx 2 \times 10^{-6}$ ohm where we have estimated for this solenoid that L = 55 μh. This evaluation of R is confirmed

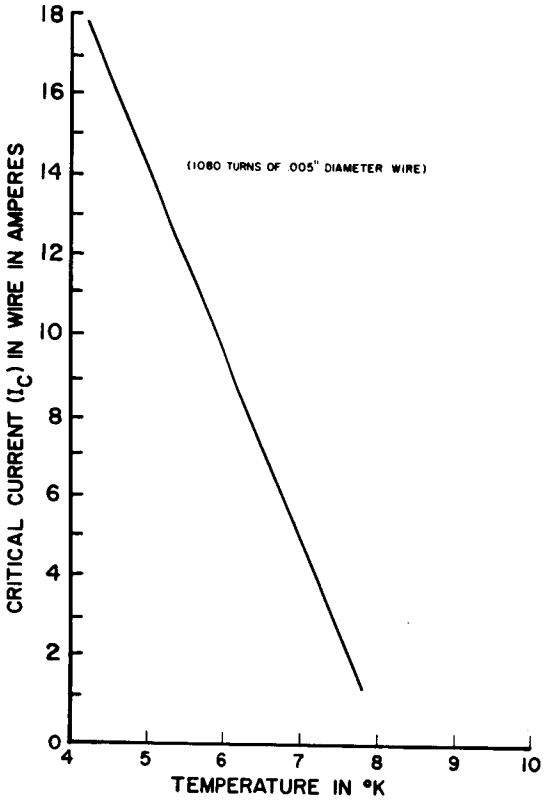

Figure 13. Critical current of NbZr solenoid.

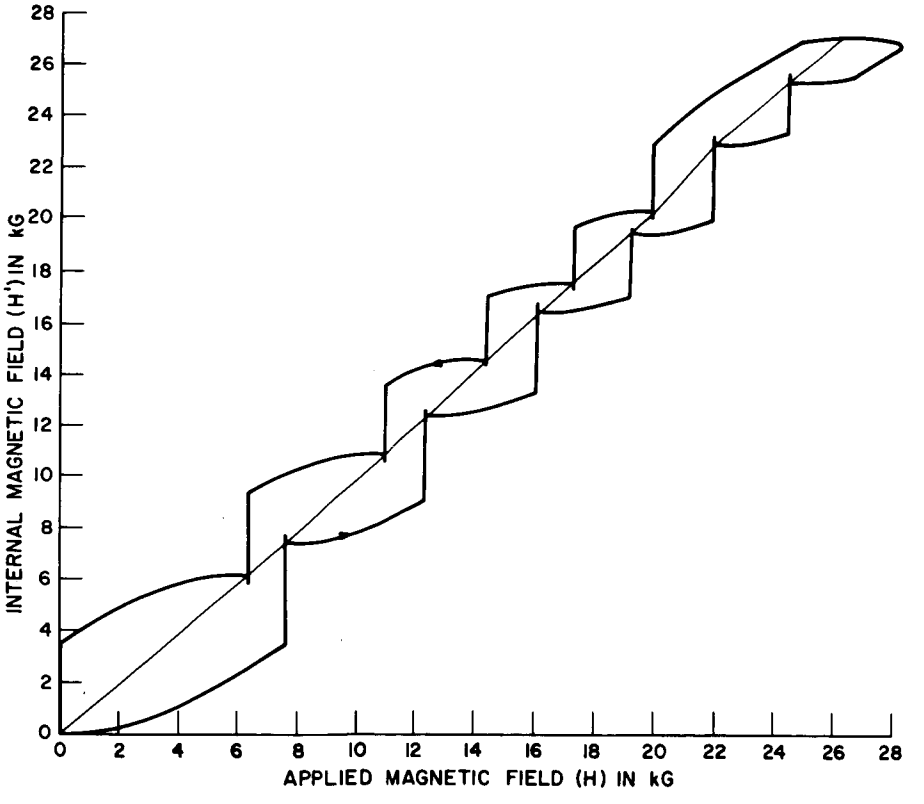

Figure 14. Magnetization of superconducting solenoid Nb_3Sn#2 at 4.9°K. (Short resistance $\approx 2 \times 10^{-6}$ ohms; dH/dt = 200 gauss/sec.)

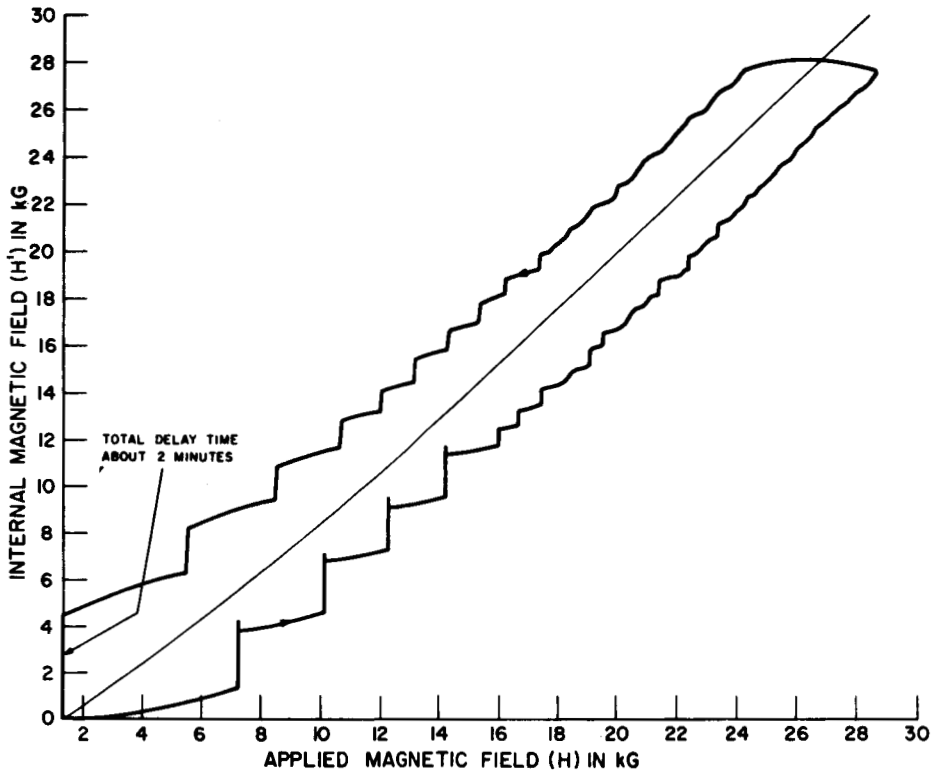

Figure 15. Magnetization of superconducting solenoid Nb_3Sn#2 at 10°K. (Short resistance $\approx 2 \times 10^{-6}$ ohms; dH/dt = 200 gauss/sec.)

by observing the decay rate of H' after the sweep is stopped. Flux jumping is also observed, but is incomplete at the higher temperatures (Figure 15). Possibly the copper cladding on the Nb_3Sn tape shunts the current past any temporarily normal spot in the tape so that the current does not completely quench before the normal spot heals itself. At sufficiently high fields, one observes something like critical state behavior in that the current decreases with increasing field. Since, however, this current depends on sweep rate, it will be less at a given field for lower sweep rates. It will be noted that just as for the solenoid NbZr #1, flux jumps are always preceded by intervals of inductive behavior, that is, flux jumps only occur when flux is not flowing across the windings.

Figure 16 shows the magnetization of solenoid Nb_3Sn #3. Because of its low value of shorting resistance ($\sim 2 \times 10^{-8}$ ohm), its magnetization was nearly

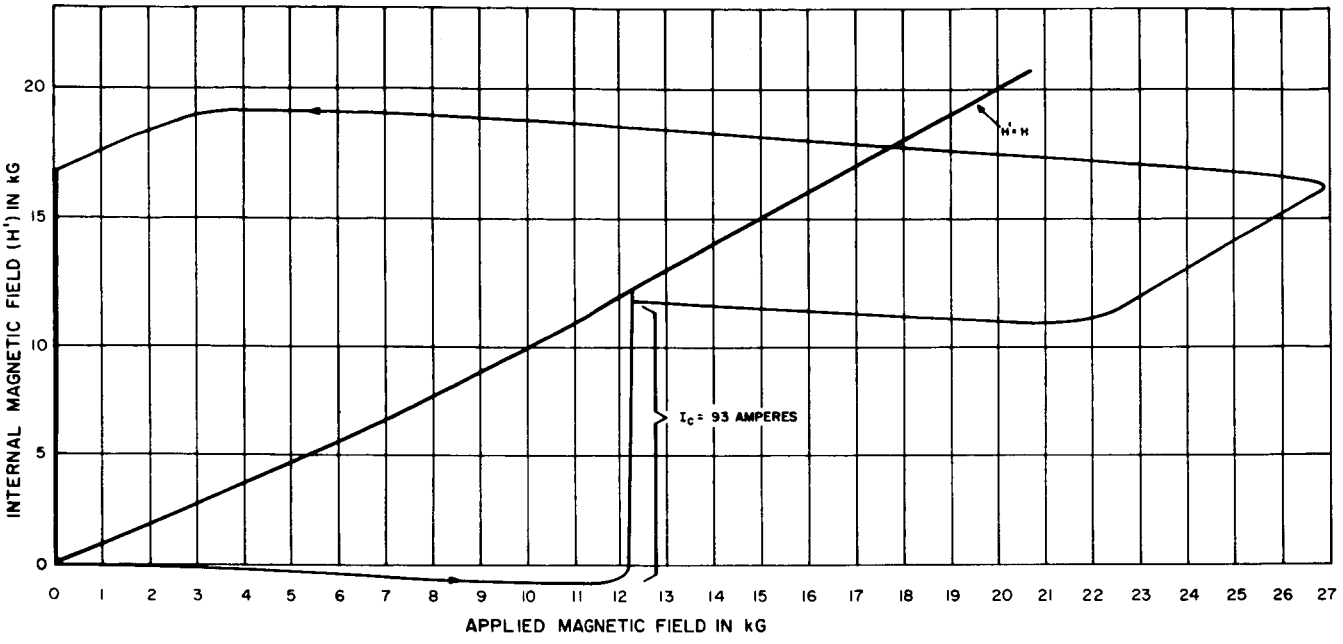

Figure 16. Magnetization of superconducting solenoid Nb_3Sn#3 at 4.2°K. (Short resistance $\approx 2 \times 10^{-8}$ ohms)

independent of sweep rate at rates between 100 G/s and 200 G/s. In keeping with this, H' exhibits the same negative slope which we have seen to be characteristic of the zero resistance solenoid. The flux jumping character differs, however, from that of solenoids NbZr #1 and Nb_3Sn #2. Flux jumps occur infrequently (not at all at higher temperatures). Furthermore, when flux jumps do occur, they are always preceded by intervals of critical state behavior, that is, by intervals of flux flow. It seems evident that different breakdown mechanisms are at work in these solenoids, but further study will be required to provide an explanation.

2. Externally Fed Solenoids

In the tests on shorted solenoids, the induced current was necessarily proportional to the applied field H when the short resistance was very small, or to dH/dt for moderately resistive shorts. By studying externally fed solenoids,

current and applied field can be separately varied, the self-field of the solenoid being relatively small. Tests were made of the critical current in solenoid NbZr #1, since it was known that currents of less than 20 amps would be sufficient. The heat leak down the current-carrying leads (#18 copper) would then be tolerable, since thermal buffers could be inserted between the copper and NbZr leads. The buffers consisted of one-inch strips of Nb_3Sn - coated Hastelloy tape, silver plated at the ends. Each NbZr lead was spot-welded to a nickel tab, which could then be soldered to a buffer; the other end of the buffer was soldered to a copper current lead. With this arrangement, the solenoid came to a temperature of 4.2°K with no current supplied to it. (Temperatures were measured with a germanium thermometer centered inside the solenoid.)

In making the tests of I_c for this solenoid, the current was set at a fixed value in zero field, a steady temperature was reached (using the heater when necessary), and the field was raised until the solenoid quenched. Below some particular value of field, which depended on temperature, I_c was independent of field (see Figure 17). We believe that in this field range the breakdown occurs at the joint between the NbZr lead and the nickel tab. At higher fields, the dependence of I_c on H for the externally fed solenoid was quite similar to the dependence of the "practical" I_c on H for the same solenoid when shorted. In the latter case, we mean by the "practical" I_c the current carried immediately prior to a flux jump, rather than the current carried in the critical state. It is possible that I_c for the externally fed solenoid could be increased above that for the shorted solenoid if the field were applied first and then the current raised. In such an arrangement, however, the temperature of the sample would be continually varying. In any case, we feel that the difficulties in keeping down the heat leak, and of ensuring that the normal-to-superconducting joints do not limit current flow, make an extension of these measurements impractical. This is particularly true of the Nb_3Sn solenoids, which have much larger values of I_c than the NbZr solenoid studied.

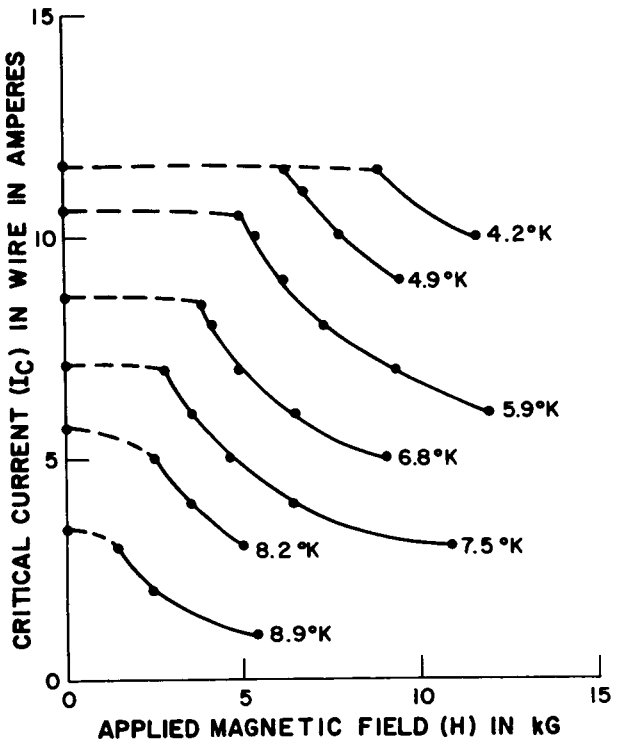

(a)

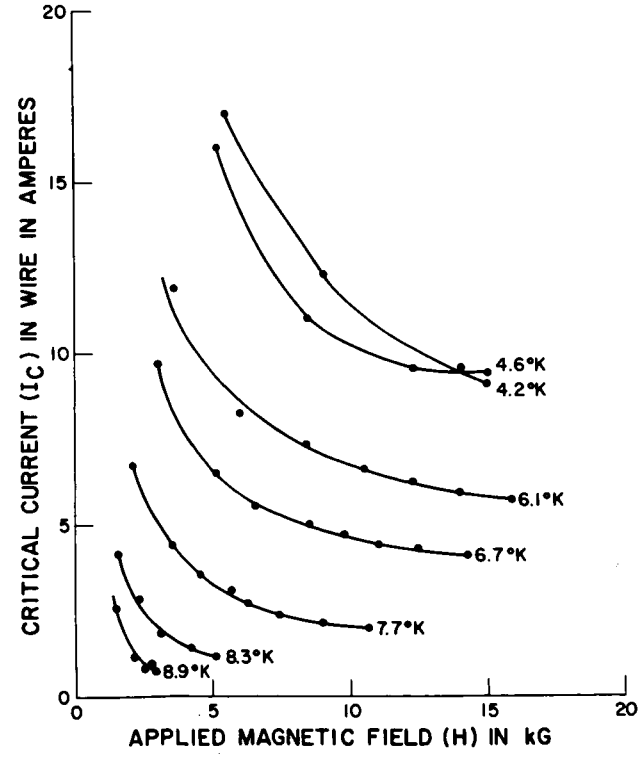

(b)

Figure 17. Comparison of "practical" I_c with externally applied I_c for NbZr solenoid: (a) I_c applied externally; (b) I_c inductively (practical I_c).

SECTION IV

SUMMARY AND RECOMMENDATIONS

This study has indicated that there exist various mechanisms which trigger flux jumping, and that a single mechanism will dominate in a given sample under particular experimental conditions of temperature, applied field, and field-sweep rate. In high J_c tubes of NbZr and of Nb_3Sn, at temperatures near 4.2°K, it appears that flux jumps are triggered deep in the sample wall. Such flux jumps occur independently of field-sweep rate (for sweep rates less than about 200 G/s and are irregularly spaced in field. Such flux jumping may well continue to indefinitely high fields at sufficiently low temperatures (see Figure 7).

As the sample temperature is increased from 4.2°K, the field interval between flux jumps (i.e., the "practical" magnetization) at first increases, but at sufficiently high temperature, the field interval between flux jumps decreases both with increasing temperature and increasing field. In this high temperature region, flux jumps occur only when the sample is carrying the full critical current density J_c throughout the wall. Furthermore, flux jumping is now rate-sensitive, the incidence of flux jumping decreasing with decreasing field-sweep rate. The mechanism triggering flux jumping has evidently changed; the mechanism is possibly now the heat liberated when Abrikosov vortices are destroyed at the tube wall surface. This explanation is suggested because the flux jumps often occur at the precise moment when the sample is about to enter the critical state, rather than after the critical state has been established.

For untreated cold-worked tubes of NbTi, flux jumping is completely absent at sufficiently low field-sweep rates. The heat treatment described in the text results in an increase in J_c, but also results in a pattern of flux jumping similar to that observed with NbZr and Nb_3Sn tubes. Furthermore, temperature cycling a heat-treated sample of NbTi lowers the "practical" J_c, i.e., decreases the field interval between flux jumps.

For shorted superconducting solenoids, we again find evidence for different mechanisms which trigger flux jumping. In both a 0.005-inch NbZr wire solenoid, and a 0.025-inch Nb_3Sn tape solenoid, it is observed that flux jumping never occurs when flux is moving freely across the windings (i.e., in the critical state); the jumps are always preceded by an interval during which no flux is moving, as evidenced by a negative slope in the H' vs H plot (see Figure 12). Furthermore, the flux jumps occur regularly at a spacing which decreases both with increasing field and with increasing temperature. At higher temperatures and fields, the flux jumps are incomplete, and finally reduce to small current excursions superimposed on the critical state. The behavior of a third solenoid, wound with 0.090-inch Nb_3Sn tape, is sharply different. For this solenoid, flux jumping occurs only when flux is moving freely across the windings. These flux jumps occur infrequently and can be eliminated at sufficiently slow sweep rates. There are similarities then in the flux jumping character of this solenoid with that of the untreated cold-worked NbTi tubes; there are also similarities in the flux jumping character of the first two solenoids with that of the NbZr and Nb_3Sn tubes.

It is evident that further study will be required to more closely characterize the flux jumping mechanisms present in high field superconductors. We propose to concentrate our efforts for the next quarter on studies of the magnetization of shorted solenoids, for these reasons:

1) Immediately useful information can be obtained about the current carrying capacity of commercially available wire. In this regard, there appears to be no particular advantage in making such measurements with externally fed samples, and considerable attendant experimental difficulties.

2) The resistance of joints between superconductors and normal metals, and more important, the effect of such joints in limiting supercurrents, can be readily measured by this method.

3) Flux jumping processes are more sharply delineated in solenoids than in tubes. As just described, we find some solenoids for which flux jumping never occurs when flux is moving freely across the windings, while for others, flux jumping occurs only when flux is moving freely across the windings. For tubes, the flux jumping processes in a given sample will vary as the experimental conditions change.

REFERENCES

1. C. P. Bean, "Magnetization of Hard Superconductors," Phys. Rev. Letters, 8, 250 (1962).

2. Y. B. Kim, C. F. Hempstead, and A. R. Strnad, "Flux Creep in Hard Superconductors," Phys. Rev., 131, 2486 (1963).

3. P. W. Anderson and Y. B. Kim, "Hard Superconductivity: Theory of the Motion of Abrikosov Lines," Rev. Mod. Phys., 36, 39 (1964).

4. J. Friedel, P. G. deGennes, and J. Matricon, "Nature of the Driving Force in Flux Creep Phenomena," Appl. Phys. Letters, 2, 119 (1963).

5. J. P. McEvoy, "Critical-State Phenomena and Flux Jumping in Niobium Stannide," R.C.A. Rev., 25, 533 (1964).

6. G. D. Cody and G. W. Cullen, "Phenomena of Superconductivity," AFML-TR-65-169, p. 27 (June, 1965).

7. C. F. Hempstead, Y. B. Kim, and A. R. Strnad, "Inductive Behavior of Superconducting Solenoids," J. Appl. Phys., 34, 3226 (1963).

ERRATA

for

Technical Summary Report
on
Contract NAS 8-11272
Titled
STUDY OF PROPERTIES OF HIGH-FIELD SUPERCONDUCTORS
AT ELEVATED TEMPERATURES

Values of magnetic field intensity given in this report are twice the true value. The following changes should be posted in the body of the report.

Page 11

Figure 4: Reduce values of horizontal and vertical scales by one half.

Line 2 of footnote:

Change 200 G/S to 100 G/S

Page 12

Paragraph 2, line 7.

Change 200 G/S and 75 to 100 G/S and 37.5

Page 13

Figure 5: Reduce horizontal and vertical scales by one half

Page 15

Figure 7: Change vertical scale values by one half. Increase slope of $\frac{dH_{c2}}{dT}$ lines by 2

Page 16

Figure 8: Reduce values of horizontal and vertical scales by one half.

Line 2:

Change 200 G/S to 100 G/S

Line 3:

Change 200 G/S to 100 G/S

Page 17

Figure 9: Reduce values of horizontal scale by one half. Increase values of vertical scale by 2.

Page 18

Figure 10: Reduce values of vertical scale by one half.

Paragraph 1, line 2:

Change 30 KG to 15 KG

Page 21

Figures 11 and 12: Reduce values of horizontal and vertical scales by one half.

Page 22

Paragraph 1, line 4:

Change 2 KG to 1 KG

Page 23

Figure 13: Reduce the values of the vertical scale by one half.

Figure 14: Reduce the values of the horizontal and vertical scales by one half.

In caption, change 200 gauss/sec to 100 gauss/sec

Page 24

Figure 15: Reduce values of horizontal and vertical scales by one half.

In caption, change 200 gauss/sec to 100 gauss/sec.

Page 25

Figure 16: Reduce values of horizontal and vertical scales by one half. Change $I_c = 93$ Amperes to $I_c = 46.5$ Amperes

Paragraph 1, line 1:

Change 100 G/S and 200 G/S to 50 G/S and 100 G/S.

Page 26

Figures 17a and 17b: Reduce values of horizontal scales to one half.

Page 28

Paragraph 1, line 6:

Change 200 G/S to 100 G/S